

The angular matching method for the muon charge sign measurement in the OPERA experiment

N. Agafonova^a, A. Aleksandrov^b, A. Anokhina^c, S. Aoki^d, A. Ariga^e, T. Ariga^e, D. Bender^f, A. Bertolin^g, C. Bozza^h, R. Brugnera^{i,g}, A. Buonaura^{b,j}, S. Buontempo^b, B. Büttner^k, M. Chernyavsky^l, A. Chukanov^m, L. Consiglio^b, N. D'Ambrosioⁿ, G. De Lellis^{b,j}, M. De Serio^{o,p}, P. Del Amo Sanchez^q, A. Di Crescenzo^b, D. Di Ferdinando^r, N. Di Marcoⁿ, S. Dmitrievski^m, M. Dracos^s, D. Duchesneau^q, S. Dusini^g, T. Dzhatdoev^c, J. Ebert^k, A. Ereditato^e, R. A. Fini^o, T. Fukuda^t, G. Galati^o, A. Garfagnini^{i,g}, G. Giacomelli^{u,r,5}, C. Göllnitz^k, J. Goldberg^v, D. Goloubkov^w, Y. Gornushkin^m, G. Grella^h, M. Guler^f, C. Gustavino^x, C. Hagner^k, T. Hara^d, A. Hollnagel^k, B. Hosseini^{b,j}, H. Ishida^t, K. Ishiguro^y, K. Jakovcic^z, C. Jollet^s, C. Kamiscioglu^{f,aa}, M. Kamiscioglu^f, J. Kawada^e, J. H. Kim^{ab}, S. H. Kim^{ab,2}, N. Kitagawa^y, B. Klicek^z, K. Kodama^{ac}, M. Komatsu^y, U. Kose^{g,1}, I. Kreslo^e, A. Lauria^{b,j}, J. Lenkeit^k, A. Ljubcic^z, A. Longhin^{ad}, P. Loverre^{ae,x}, A. Malgin^a, M. Malenica^z, G. Mandrioli^r, T. Matsuo^t, V. Matveev^a, N. Mauri^{u,r}, E. Medinaceli^{i,g}, A. Mereaglia^s, M. Meyer^{k,*}, S. Mikado^t, P. Monacelli^{af}, M. C. Montesi^{b,j}, K. Morishima^y, M. T. Muciaccia^{o,p}, N. Naganawa^y, T. Naka^y, M. Nakamura^y, T. Nakano^y, Y. Nakatsuka^y, K. Niwa^y, S. Ogawa^t, N. Okateva^l, A. Olshevsky^m, T. Omura^y, K. Ozaki^d, A. Paoloni^{ad}, B. D. Park^{ab,3}, I. G. Park^{ab}, L. Pasqualini^{u,r}, A. Pastore^o, L. Patrizi^r, H. Pessard^q, C. Pistillo^e, D. Podgrudkov^c, N. Polukhina^l, M. Pozzato^{u,4}, F. Pupilliⁿ, M. Roda^{i,g}, H. Rokujo^y, T. Roganova^c, G. Rosa^{ae,x}, I. Rostovtseva^w, O. Ryazhskaya^a, O. Sato^y, Y. Sato^{ag}, A. Schembriⁿ, I. Shakiryanova^a, T. Shchedrina^b, A. Sheshukov^b, H. Shibuya^t, T. Shiraishi^y, G. Shoziyoev^c, S. Simone^{o,p}, M. Sioli^{u,r}, C. Sirignano^{i,g}, G. Sirri^r, M. Spinetti^{ad}, L. Stanco^g, N. Starkov^l, S. M. Stellacci^h, M. Stipcovic^z, P. Strolin^{b,j}, S. Takahashi^d, M. Tenti^r, F. Terranova^{ad,ah}, V. Tioukov^b, S. Tufanli^e, P. Vilain^{ai}, M. Vladimirov^l, L. Votano^{ad}, J. L. Vuilleumier^e, G. Wilquet^{ai}, B. Wonsak^{k,*}, C. S. Yoon^{ab}, Y. Zaitsev^w, S. Zemskova^m, A. Zghiche^q

^aINR Institute for Nuclear Research, Russian Academy of Sciences RUS-117312, Moscow, Russia

^bINFN Sezione di Napoli, I-80125 Napoli, Italy

^cSINP MSU-Skobel'syn Institute of Nuclear Physics, Lomonosov Moscow State University, RUS-119992 Moscow, Russia

^dKobe University, J-657-8501 Kobe, Japan

^eAlbert Einstein Center for Fundamental Physics, Laboratory for High Energy Physics (LHEP), University of Bern, CH-3012 Bern, Switzerland

^fMETU Middle East Technical University, TR-06531 Ankara, Turkey

^gINFN Sezione di Padova, I-35131 Padova, Italy

^hDip. di Fisica dell'Uni. di Salerno and "Gruppo Collegato" INFN, I-84084 Fisciano (SA) Italy

ⁱDipartimento di Fisica dell'Università di Padova, I-35131 Padova, Italy

^jDipartimento di Scienze Fisiche dell'Università Federico II di Napoli, I-80125 Napoli, Italy

^kHamburg University, D-22761 Hamburg, Germany

^lLPI-Lebedev Physical Institute of the Russian Academy of Sciences, 119991 Moscow, Russia

^mJINR-Joint Institute for Nuclear Research, RUS-141980 Dubna, Russia

ⁿINFN-Laboratori Nazionali del Gran Sasso, I-67010 Assergi (L'Aquila), Italy

^oINFN Sezione di Bari, I-70126 Bari, Italy

^pDipartimento di Fisica dell'Università di Bari, I-70126 Bari, Italy

^qLAPP, Université Savoie Mont Blanc, CNRS/IN2P3, F-74941 Annecy-le-Vieux, France

^rINFN Sezione di Bologna, I-40127 Bologna, Italy

^sIPHC, Université de Strasbourg, CNRS/IN2P3, F-67037 Strasbourg, France

^tToho University, J-274-8510 Funabashi, Japan

^uDipartimento di Fisica e Astronomia dell'Università di Bologna, I-40127 Bologna, Italy

^vDepartment of Physics, Technion, IL-32000 Haifa, Israel

^wITEP-Institute for Theoretical and Experimental Physics, RUS-317259 Moscow, Russia

^xINFN Sezione di Roma, I-00185 Roma, Italy

^yNagoya University, J-464-8602 Nagoya, Japan

^zIRB-Rudjer Boskovic Institute, HR-10002 Zagreb, Croatia

^{aa}Ankara University, TR-06100 Ankara, Turkey

^{ab}Gyeongsang National University, ROK-900 Gazwa-dong, Jinju 660-701, Korea

^{ac}Aichi University of Education, J-448-8542 Kariya (Aichi-Ken), Japan

^{ad}INFN-Laboratori Nazionali di Frascati dell'INFN, I-00044 Frascati (Roma), Italy

^{ae}Dipartimento di Fisica dell'Università di Roma 'La Sapienza' and INFN, I-00185 Roma, Italy

^{af}Dipartimento di Fisica dell'Università dell'Aquila and INFN, I-67100 L'Aquila, Italy

*Corresponding authors

Universität Hamburg, Luruper Chaussee 149, 22761 Hamburg, Germany

Email addresses: mikko.meyer@desy.de (M. Meyer), bwonsak@mail.desy.de (B. Wonsak)

¹Now at CERN, Geneva, Switzerland

²Now at CUP, Institute for Basic Science, Daejeon, Korea.

³Now at Samsung Changwon Hospital, SKKU, Changwon, Korea.

⁴Now at Dipartimento di Fisica, Università degli Studi di Trento

⁵deceased

Abstract

The long baseline neutrino oscillation experiment OPERA has observed the direct appearance of ν_τ in the CNGS ν_μ beam. The task of the two muon magnetic spectrometers of the detector is to identify muons produced in the tau lepton decay and in ν_μ CC interactions, and measure their charge and momentum. Apart from the kinematic analysis of muonic tau lepton decays, this helps in reducing the background resulting from the decay of charmed particles produced in ν_μ CC interactions. In the new method for the charge sign determination described below, a weight based on the angular matching between straight track segments reconstructed on both sides of a dipole magnet arm is attributed to each of up to four charge sign measurements. Results based on the analysis of Monte Carlo simulated and real data are presented. They are compared to those produced by the method used so far where weights are based on the precision on the measurement of the track segment angles. A significant reduction of up to 40% of the fraction of wrongly determined charges is obtained.

Keywords: Neutrino, OPERA, Drift Tube, Muon Charge Sign, Spectrometer

1. Introduction

The OPERA experiment has been designed to observe the direct appearance of ν_τ in a ν_μ beam by resolving the track left by the short-lived τ^- lepton emitted in their CC interactions [1]. Four candidate events have been observed so far after $\sim 75\%$ of the data have been analysed [2–5]. The significance of the observation amounts to 4.2σ [5]. Identifying primary muons is of utmost importance in order to reduce background processes arising from topologically similar decays of charmed particles induced in ν_μ CC interactions. In case the charmed particle decays into a muon, $\nu_\mu N \rightarrow (c \rightarrow \mu^+ X) \mu^- Y$, background may be further reduced by identifying the secondary muon and determining the positive sign of its charge. OPERA expects to observe about one $\nu_\tau N \rightarrow (\tau^- \rightarrow \mu^- \bar{\nu}_\mu \nu_\tau) Y$ event assuming full $\nu_\mu - \nu_\tau$ mixing and $\Delta m_{32}^2 = 2.34 \times 10^{-3} \text{ eV}^2$ [6]. It is therefore mandatory to have an efficient estimator of the muon charge sign and also to have an indicator of its quality on an event by event basis.

The use of a magnetic spectrometer enables the measurement of the particle charge and momentum in high energy physics. The OPERA experiment [7] uses drift tube detectors to measure the directions of straight track segments along the muon trajectory in front of and behind the magnetized regions [8].

In the procedure used so far, the quality of the charge sign determination relies on the combination of weights computed for each charge measurement unit (CMU) and is based on the precision on the angles of the two track segments that constitute the muon trajectory at the entry and the exit of the magnet arm in the plane of curvature. More information on this procedure referred to below as the OPERA Standard Method (OSM) is given in appendix A. In this paper, we present a new method to weigh the charge sign determination in each CMU based on the quality of the matching between these two angles, assuming a circular trajectory inside the magnet. In the following we refer



Figure 1: Side view of one of the two OPERA spectrometers. See also Figure 2.

to it as the Angular Matching Method (AMM). The OPERA detector has two spectrometers, each with two CMU and up to four weights may thus be combined. The results based on Monte Carlo simulations (MC) are presented and the potential of the AMM is demonstrated. Finally a test with real data is performed and a first estimation of the impurity (defined as the fraction of muons for which the charge sign is wrongly deter-

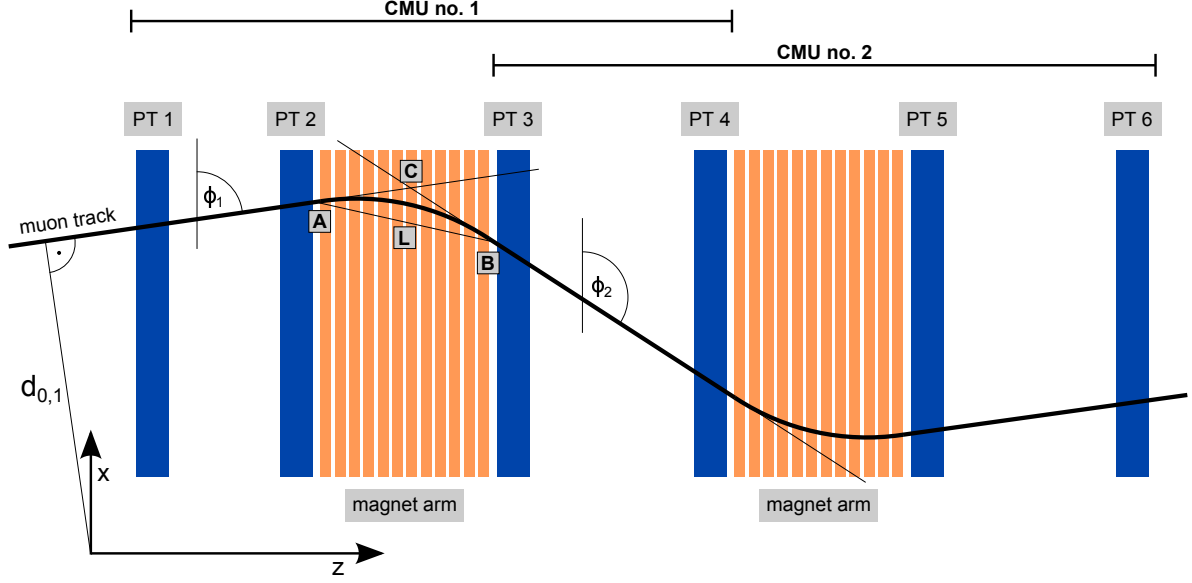


Figure 2: Schematic top view of one of the two OPERA spectrometers. The six Precision Tracker (PT) planes are used for the track reconstruction. Each charge measurement unit (CMU) delivers a measurement of charge/momentum, provided the track is reconstructed on both sides of the magnet arm. PT1-PT4 form the first CMU and PT3-PT6 form the second CMU. The charge sign determination in the first CMU uses the deflection angle $\Delta\phi = \phi_2 - \phi_1$. The OPERA detector has a total of four CMUs, two per spectrometer.

mined) for one spectrometer is given using the AMM.

2. The OPERA detector

OPERA is a hybrid detector composed of electronic detectors and nuclear emulsions located at the Laboratori Nazionali del Gran Sasso (LNGS) in Italy [7]. It has been exposed between spring 2008 and December 2012 to the CERN to Gran Sasso (CNGS) ν_μ beam with an average energy of 17 GeV [9]. The contaminations of $\bar{\nu}_\mu$, ν_e and $\bar{\nu}_e$ CC interactions, relative to ν_μ CC interactions, are 2.1%, 0.9% and less than 0.1%, respectively [10]. The prompt ν_τ contamination is negligible. The collected data correspond to about 18×10^{19} protons on target and a total of 19505 neutrino interactions have been recorded.

The design of the detector takes two conflicting requirements into account: a large target mass to cope with the minute neutrino interaction cross-section and the baseline, and a micro-metric resolution to allow the detection of the short-lived τ lepton. The total target mass is about 1.2 kt. The target is made of approximately 150,000 basic units called bricks each consisting of 56 lead plates of 1 mm thickness that provide the mass, interleaved with nuclear emulsion films that provide the spatial resolution. Bricks are assembled in walls interleaved with the Target Tracker (TT): 62 pairs of planes of horizontal and vertical plastic scintillator strips having their signal collected by wave length shifting fibres and read by multi-anode photomultiplier tubes. They are aimed at triggering the data acquisition, measuring the trajectories of charged particles through the target, locating bricks where neutrino interactions occurred and providing coarse calorimetric information. The instrumented target is divided into two identical supermodules (SM). Downstream

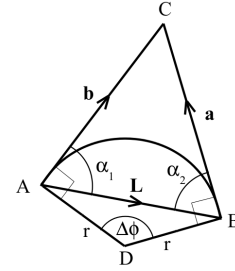
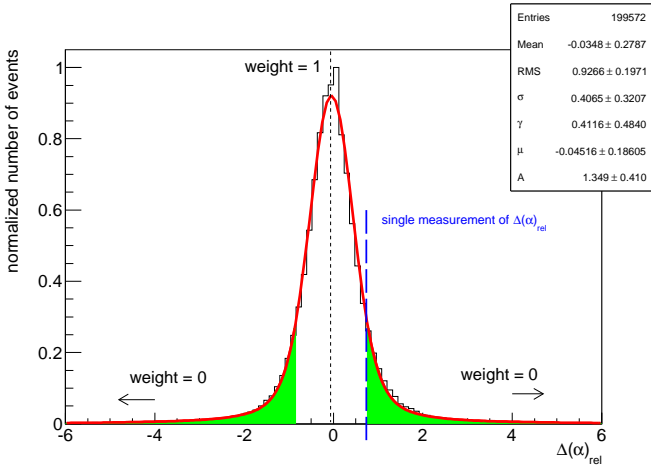


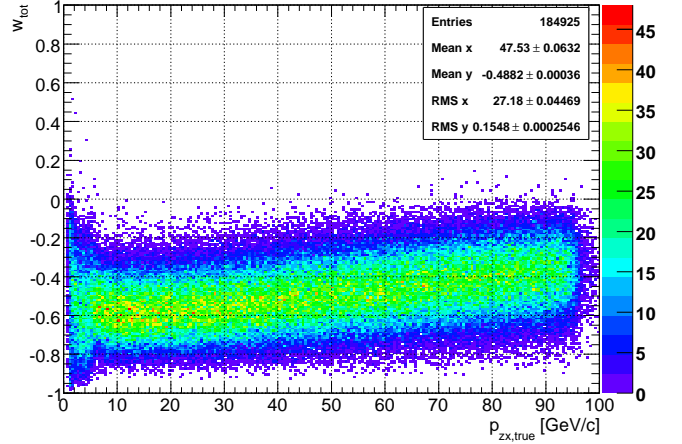
Figure 3: The particle trajectory in the magnetic field is shown (arc of a circle AB of radius r). Vectors **a** and **b** (intersecting at C) are tangents to the circular path at the entry (A) and exit (B) points. A, B and C refer to points in Figure 2. $\Delta\phi = \phi_2 - \phi_1$ is the deflection angle.

of each of these, a magnetic spectrometer identifies and measures the momentum and the charge of the penetrating muons. The dipole magnet arms are instrumented internally by planes of resistive plate chambers (RPC) and externally by stations of high precision vertical drift tubes walls called the Precision Tracker (PT) [11] (see Figure 1). The 1.53 T magnetic field is oriented vertically. Non-uniformities in the magnetic field strength have been measured to be less than 3% [7].

Each CMU (see Figures 1 and 2) is composed of two drift tube walls in front of and behind a magnet arm. The CMU delivers a measurement of charge and momentum in the horizontal projection, provided the track is reconstructed on both sides of the magnet arm. The spatial resolution of the PT is better than $300 \mu\text{m}$ in the horizontal plane [11, 12] and allows



(a) Charge weight principle



(b) Charge weight dependence on momentum

Figure 4: (a): The black histogram shows the distribution of the relative angular deviations $\Delta(\alpha)_{rel}$ (Eq. 1) and the red curve the Voigtian distribution that best fits to it. The values obtained for its parameters μ , σ and γ are shown in the box. A is a normalization factor. The mean value μ is indicated by the dashed line. The weight w_i attributed to the charge sign measurement obtained in a single CMU i is given by the integral defined by Eq. (4), (5) and (6). It corresponds to the green area. The smaller $\Delta(\alpha)_{rel}$ is, the larger is the weight. Figure (b) shows, for simulated μ^- , the dependence of the total weight w_{tot} (Eq. (8)) on the true Monte Carlo momentum $p_{zx,true}$ projected in the horizontal plane. The sign of w_{tot} fixes the sign of the reconstructed muon charge (see Section 4.2). For both figures the simulation method MC-I is used with negative muons (see Section 3), except that, for Figure (b), the momentum is uniformly distributed between 1 and 100 GeV/c instead of by steps of 1 GeV/c.

determining the sign of the muon charge for momenta of up to 25 GeV/c with an efficiency of more than 99%. At this point, it is necessary to stress that in the single event observed so far in this decay channel [4], the low momentum muon stops in the first magnet arm and its charge may thus not be measured by the PT. Instead, the hits recorded by RPC that instrument the magnet arm have been used to reconstruct the negative sign of the muon track curvature with a probability of 5.6σ [4]. Any improvement in algorithms using PT data for charge sign determination can therefore not affect the analysis of this particular event.

3. Monte Carlo simulations

Two different Monte Carlo simulations based on GEANT3 [13] have been used. For both types of simulation, muon trajectories have been reconstructed and their momenta evaluated using the full OPERA analysis chain [14].

The first MC simulation (MC-I) is used to demonstrate the performances of the AMM. The sample consists of positive and negative muons emitted at the centre of the targets of SM1 or of SM2 at an angle orthogonal to the drift tubes planes. The momentum was varied between 1 and 100 GeV/c by steps of 1 GeV/c. The angle is close to those of most muons produced in CNGS CC neutrino interactions in the detector.

The second MC setup (MC-II) is based on the event generator NEGN [15], developed in the framework of the NOMAD experiment [16]. The OPERA simulation chain, including the

CC interactions of the CNGS neutrinos and the responses of the electronic detectors, has been used to simulate the second sample.

4. Methodology

4.1. Identification of track inconsistencies

The straight track segments reconstructed by the PT provide track parameters projected in the horizontal plane (x, z) with z along the horizontal projection of the beam line and x parallel to the PT walls. For detailed information on track reconstruction in the PT see [8]. Two segments on each side $j = 1, 2$ of a magnet arm are described by the angles ϕ_j that they enclose with axis x and by their distance $d_{0,j}$ to the reference frame origin (see Figure 2; for reasons of simplicity $d_{0,2}$ is not shown in the figure). $\Delta\phi = \phi_2 - \phi_1$ is the deflection angle. If energy loss and multiple scattering are neglected, a charged particle trajectory in the magnetic field is an arc of a circle tangent to both track segments at their magnet arms entry/exit points (see Figure 3). Calling α_j the complement of the angle between the chord joining these two points and track segment j (see Figure 3), it follows that $\alpha_1 = \alpha_2$ and $\Delta\phi = \alpha_1 + \alpha_2$. See Appendix B for more details. The relative angular deviation in CMU i

$$\Delta(\alpha)_{rel,i} = 2 \frac{\alpha_1 - \alpha_2}{\alpha_1 + \alpha_2} \Big|_i = 2 \frac{\alpha_1 - \alpha_2}{\Delta\phi} \Big|_i \quad (1)$$

provides a measurement of the mismatch between the two reconstructed track segments. The more α_1 differs from α_2 , the

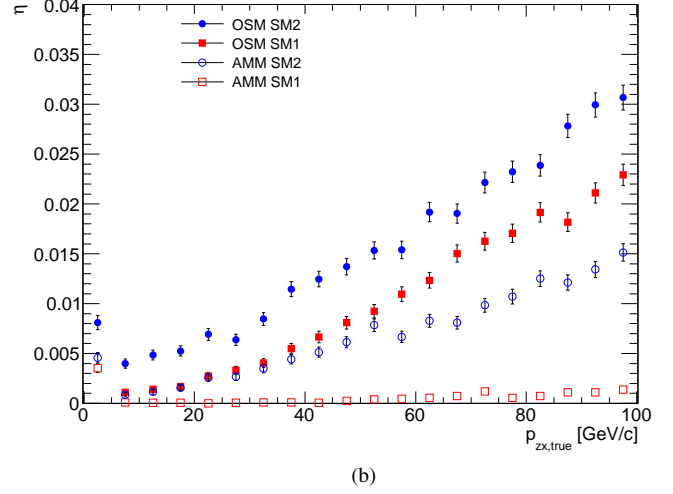
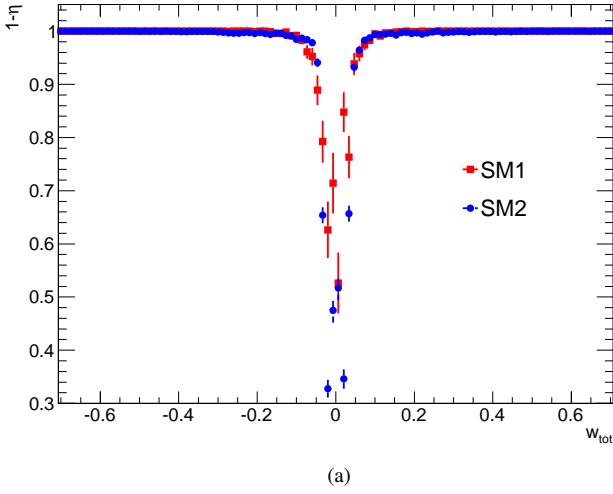


Figure 5: Purity $1 - \eta$ dependence on the total weight w_{tot} . The vertex of the incoming muons was set in the middle of the target section, respectively in the first (SM1) and in the second supermodule (SM2). The impurity η dependence on the momentum $p_{zx,true}$ is shown in (b). The simulation method is MC-I.

greater the likelihood is that one or both of the track segments are reconstructed with poor precision, in which case they may also be wrongly associated, yielding to a wrong muon sign determination.

In the following a weight is constructed such that large angular deviations result in a small weight.

The distribution of the reconstructed $\Delta(\alpha)_{rel}$ for 200,000 negative muons simulated following MC-I (see Section 3) is shown in Figure 4a. It has been fitted with a Voigtian distribution $V(x)$, the convolution of a Gaussian $G(x)$ and a Lorentzian $L(x)$ distribution:

$$V(x) = G(x) \otimes L(x) \quad (2)$$

$$= A \frac{1}{\sqrt{2\pi}\sigma} e^{-\frac{1}{2}\left(\frac{x-\mu}{\sigma}\right)^2} \otimes \frac{1}{2\pi} \frac{\gamma}{(x-\mu)^2 + \frac{1}{4}\gamma^2}, \quad (3)$$

where $\mu = 0.05 \pm 0.19$, $\gamma = 0.41 \pm 0.48$ and $\sigma = 0.41 \pm 0.32$ receive their values from the fit; as given in the box of Figure 4a. A is a normalization factor. As anticipated, the mean value μ is fully compatible with 0. The relative error on the angle difference that results from the precision on their measurement is well reproduced by a Gaussian distribution except for long tails that are described by the convolution with a Lorentzian distribution. The quality of the track reconstruction in CMU i is given by its weight

$$w_i = 1 - \int_{a_i}^{d_i} V(\Delta(\alpha)_{rel,i}) d\Delta(\alpha)_{rel,i}. \quad (4)$$

The integration limits are

$$d_i = \mu + |\Delta(\alpha)_{rel,i} - \mu| \quad (5)$$

$$a_i = \mu - |\Delta(\alpha)_{rel,i} - \mu|. \quad (6)$$

For $\Delta(\alpha)_{rel,i} \approx \mu$ a weight of ~ 1 is attributed to the measurement, while it approaches 0 for large values of $|\Delta(\alpha)_{rel,i}|$ (Figure 4a).

4.2. Charge sign determination

The OPERA detector consists of four CMU each allowing the determination of the deflection angle $\Delta\phi$. For muons created in CNGS neutrino interactions, taking into account the polarity P_i of the magnetic field in CMU i , the charge sign c_i is given by

$$c_i = \frac{\phi_{i2} - \phi_{i1}}{|\phi_{i2} - \phi_{i1}|} P_i, \quad (7)$$

where ϕ_{ij} represents the reconstructed angle in front of ($j = 1$) and behind ($j = 2$) the magnet arm of CMU i . The average total weight w_{tot} evaluates to

$$w_{tot} = \frac{1}{n} \cdot \sum_{i=1}^n c_i \cdot w_i, \quad (8)$$

where n denotes the number of used CMU. The sign of w_{tot} is the reconstructed particle charge sign. Figure 4b shows the average total weight w_{tot} as a function of the true MC momentum projected in the horizontal plane $p_{zx,true}$ for simulated negative muons. Reconstructed muons with $w_{tot} > 0$ have the sign of their charge misidentified. The momentum dependence of the wrong sign determination is small and further discussed in Section 5. This is an important advantage in comparison with conventional methods in particle physics as these are strongly momentum dependent (e.g. Kalman tracking [17]). The width of the w_{tot} distribution is dominated by the measurement errors on the angles and is essentially momentum independent except at low momentum where the muon trajectory inside the magnets is modified by multiple Coulomb scattering.

Table 1: Comparison between the total impurities averaged over the momentum range 1-100 GeV/c obtained with the new AMM and the OSM.

Vertex position	η_{OSM} (all) [%]	η_{AMM} (all) [%]
target of SM1	1.35 ± 0.02	0.06 ± 0.01
target of SM2	1.55 ± 0.02	0.69 ± 0.01
all	1.45 ± 0.01	0.37 ± 0.01

5. Charge misidentification results

5.1. Performances of AMM

To demonstrate the potential of the new charge sign algorithm the simulation MC-I was used and the impurity η as well as the efficiency ε for μ^+ and μ^- were calculated. The impurity is defined by

$$\eta = \frac{n_w}{n_c} \quad (9)$$

where n_w is the number of wrong charge sign determinations, while n_c is the total number of charge sign assignments. If a cut on the total weight w_{tot} is applied the discarded events are not included in n_c and n_w . The efficiency is defined by $\varepsilon = n/n_p$, where $n = n_c - n_w$ is the number of correct charge sign assignments and n_p the number of possible charge sign assignments, where at least one CMU is crossed by the particle. If no cut is applied to w_{tot} then $\eta = 1 - \varepsilon$.

It is anticipated that, at very low momentum, purity and efficiency will suffer from the multiple Coulomb scattering inside the magnet and, at very high momentum, from the limited resolution of the PT. A cut on the weight w_{tot} will increase the purity as shown in Figure 5a at the cost of a reduction of the efficiency. The results obtained for the impurity are shown in Table 1 and in Figure 5b for both OSM and AMM. The following observations are made for the AMM:

- Even in the absence of cuts on the weight w_{tot} , the impurity remains smaller than 0.1% at momenta larger than 5 GeV/c, if the vertex is set in the target of SM1. In the momentum range considered in the search for ν_τ candidate events, $p_\mu < 15$ GeV/c, it does not exceed 0.01% except for momenta smaller than 5 GeV/c where it increases to 0.4% (Figure 5b).
- If the vertex is set in the target of SM2 the impurity increases, but still does not exceed 1.6% at high momentum and 0.2% for $5 \text{ GeV/c} < p_\mu < 15 \text{ GeV/c}$. For $p_\mu < 5 \text{ GeV/c}$ it increases to 0.5% (Figure 5b).

A cut on the weight at $|w_{tot}| > 0.1$ (0.2) removes most of the impurities if the vertex is set in the target of SM1 even at very low or very high momentum at the cost of a reduction in the efficiency as large as 10 % at very high momentum. For $5 \text{ GeV/c} < p_\mu < 15 \text{ GeV/c}$, however, the efficiency remains larger than 99.7% but it falls to 99% (96%) for $p_\mu < 5 \text{ GeV/c}$ when a cut on the weight is applied.

The already small fraction of wrong charge sign determination obtained with the OSM is reduced by an order of magnitude

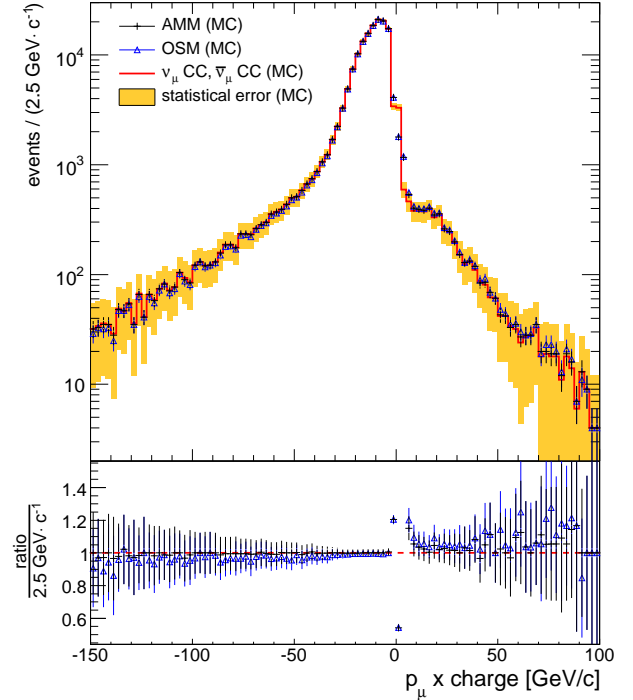


Figure 6: Top: reconstructed (anti-)muon momentum multiplied with the sign of its charge for simulated CNGS CC neutrino interactions (MC-II). The charge is the MC truth (red histogram) or the charge reconstructed with either OSM (blue histogram with triangle) or AMM (black histogram with vertical mark). For visibility, the statistical error (orange band) on the first spectrum (MC truth sign) has been multiplied by 3. Bottom: ratios between the above spectrum using the MC truth charge sign and respectively the two above spectra using the reconstructed charge signs obtained by the OSM and AMM.

when the vertex is placed in the target of SM1 and by a factor of 4 on average. The potential impact of this improvement on the physics results of OPERA is discussed in Section 7.

5.2. Simulation of CNGS neutrinos CC interactions

A sample of CNGS beam CC neutrino interactions has been generated in the detector target, using the full OPERA simulation chain MC-II described above [14]. Figure 6 shows the distribution of the MC value of the product of the reconstructed muon momentum p_μ and its charge in a range extending from -150 GeV/c to 100 GeV/c that includes essentially all events. The fraction of μ^+ in the total sample of muons estimated with the AMM and the OSM are $(3.7 \pm 0.1(\text{stat.}))\%$ and $(3.9 \pm 0.1(\text{stat.}))\%$, respectively. The estimated fraction of μ^+ , mainly emitted in CC interactions of $\bar{\nu}_\mu$ from beam contamination, may only be biased towards values larger than the MC truth, $(3.4 \pm 0.1(\text{stat.}))\%$. The fraction of incorrect charge assignments is reduced by ~40%, from 0.5% to 0.3%, with AMM.

Figure 7 shows the muon charge determination impurity as a function of the momentum in the range $2 \text{ GeV/c} < p_\mu < 150$

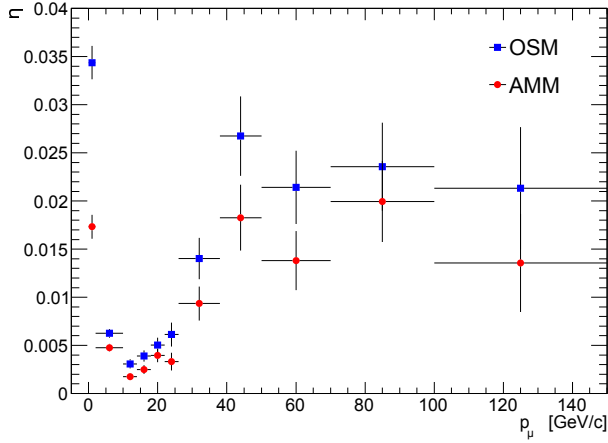


Figure 7: Dependence on the muon momentum p_μ of the impurity η on the charge sign determination for simulated CNGS CC neutrino interactions (MC-II).

GeV/c obtained with both methods. Compared to the OSM, $\eta_{OSM} = (1.06 \pm 0.04 \text{ (stat.)})\%$, the impurity obtained with the AMM is reduced by $\sim 41\%$, $\eta_{AMM} = (0.62 \pm 0.03 \text{ (stat.)})\%$, if a maximum momentum cut is applied at 15 GeV/c. If a cut $|w_{tot}| > 0.1$ is applied to the charge determination, the impurity is reduced by a factor of 3, while the efficiency is reduced to $\sim 86\%$.

6. Charge misidentification for real data

In order to test the new method with real data, two investigations were carried out.

Neutrino interactions were selected in which the muon propagates through both spectrometers (number of used CMU $n_{CMU} = 4$) having one charge measurement in disagreement with the other three measurements. The single sign measurement is more likely to be incorrect than the other three measurements. Figure 8 shows as an example the weight of the one station in disagreement, $w_{disagree}$. Compared to $|w_{agree}|$, $|w_{disagree}|$ is most often very small, $|w_{disagree}| < 0.2$.

The aim of the second investigation is to estimate the impurity η_{SM} for muons crossing one complete spectrometer ($n_{CMU} = 2$). For that purpose, the data sample with particles crossing both spectrometers is used ($n_{CMU} = 4$). It has been verified that all four CMU have equal systematics [12, 18] and therefore an equal impurity η_{SM} is expected for both spectrometers. The fraction of tracks with a different charge sign measurement in both spectrometers is then given by

$$\frac{n^{+-}}{n} = 2\eta_{SM}(1 - \eta_{SM}), \quad (10)$$

where n is the total number of muons and n^{+-} is the number of events where different charge signs are obtained. The charge sign for each spectrometer is reconstructed independently by taking the weighted average of the two measurements. Figure 9

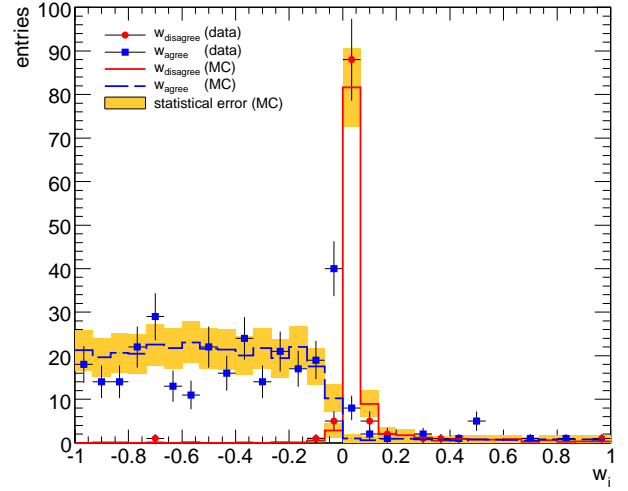
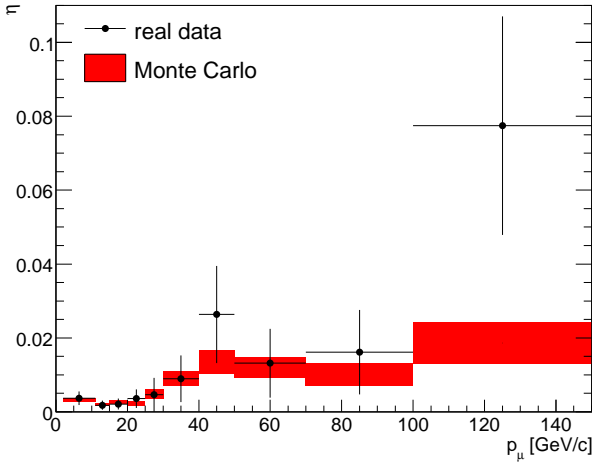


Figure 8: Real data and MC comparison: Tracks were used which propagated through all four charge measurement units and where three stations are in agreement and one station is in disagreement. w_{agree} is the weight of the stations in agreement while $w_{disagree}$ is the weight of the station in disagreement. This station is expected to have more often delivered a wrong charge sign, and indeed it yields a small absolute value of the weight.

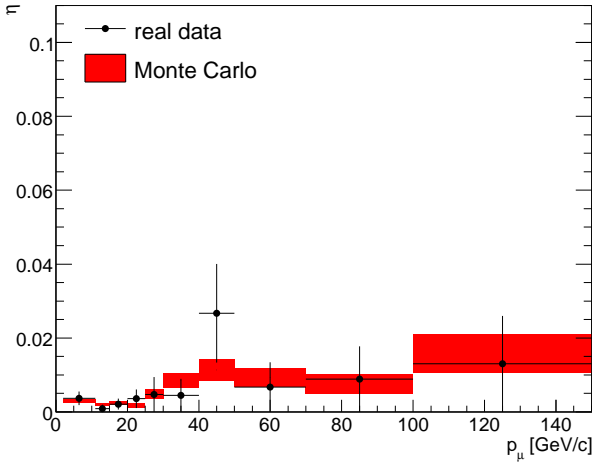
shows the impurity in the muon charge determination for real data obtained by this method as a function of momentum. It is compared to the MC predictions. The impurity is kept below 0.5% and the muon charge is correctly determined with an efficiency larger than 99.5% for momenta below 15 GeV/c, the momentum range relevant for the study of $\nu_\mu \rightarrow \nu_\tau$ oscillations (Figure 9a). An additional cut at $|w_{tot}| > 0.1$ allows a further reduction of the impurity at the cost of an increase of the fraction of sign indetermination (Figure 9b). This result is relevant for most of the OPERA events as in 80% of the CC interactions, the muon crosses at least one full spectrometer. In 35% of the cases, both spectrometers are crossed, which allows a further reduction of the impurity.

7. Conclusion and outlook

A new method (AMM) has been developed in the framework of the OPERA experiment to improve the determination of the muon charge sign in the spectrometers. In each measurement unit a weight is assigned to the matching between the measured angles of the two straight track segments at the entry and exit of the magnet arm, projected in the plane of curvature. These weights are then combined into a global weight, the sign of which determines the sign of the charge. Its modulus measures the quality of this determination. A lower cut applied to the weight improves the purity - the fraction of correct charge sign determinations - at the cost of some reduction in the efficiency, the fraction of muons for which the charge is determined. The purity naturally increases with the number



(a) No cut.



(b) Cut at $|w_{tot}| > 0.1$.

Figure 9: Evaluation of the impurity η with real data compared to the MC expectation as a function of the muon momentum p_μ for one SM using the AMM (Eq. 8). The red band corresponds to the $\pm 1\sigma$ statistical uncertainty. The simulation method is MC-II. In Figure 9a no cut is applied on the weight. In Figure 9b a cut is applied at $|w_{tot}| > 0.1$.

of CMUs that are traversed by the muon. It has only a small momentum dependence and is affected by two irreducible effects: at small momentum by the multiple Coulomb scattering suffered by the muon inside the magnet and, at high momentum and small deflection, by the finite resolution in the measurement of the track segment angles.

The AMM has been used to evaluate the purity in the charge sign measurement by one spectrometer for real CNGS beam data by comparing how often both spectrometers measure the same sign. The impurity is kept below 0.5% in the momentum range relevant for the OPERA main analysis.

The AMM analysis is part of a campaign of studies to reduce the backgrounds for the OPERA experiment. The impact

of the AMM tool on the ν_τ appearance analysis is at present to some extent limited by the fact that the background in the muonic channel is only partially composed of charm decays (20%) and that it represents only 1.3% of the background in all decay channels. Nevertheless the estimate of the dominant background in the muonic channel (large-angle muon scattering) is presently based on conservative assumptions. Ongoing studies might reduce it to a level that would imply a more significant role for the charm background reduction achieved with the AMM algorithm.

The use of the AMM is not restricted to the configuration of the OPERA spectrometers and may be easily adapted to other experiments, for example to decrease the fraction of CC events with wrong muon charge sign determination or to better control the systematics in the separation between ν_μ and $\bar{\nu}_\mu$ CC interactions. Experiments with point-like track measurements in the magnetic field (e.g. [19]) may adapt the method for their purposes by using three points to form the triangle shown in Figure 3 instead of two tangents. Further possible applications of the AMM are momentum determination and alignment of measurement units.

Appendix A

The OSM used so far by the OPERA experiment for the charge sign determination is described in detail in [20].

In each CMU i , a weight w_i is computed that takes account of the measurement precision of the angles ϕ_1 and ϕ_2 made by the two track segments with the transverse direction x in the horizontal plane of projection, the plane of curvature.

$$w_i = \frac{\phi_2 - \phi_1}{\sqrt{\sigma_{\phi_1}^2 + \sigma_{\phi_2}^2}} \quad (\text{A.1})$$

If all signs are equal, this sign represents the result. The weights of each measurement are added in quadrature to form a global weight for the output. If the signs differ, the sign measured by the majority of the CMU is used. Only the weights of the stations belonging to the majority are used and added up for the output. If an equal number of positive and negative signs is obtained, it is assumed, that the measurement is disturbed by the presence of additional hits due to the leakage of the tail of the hadronic and electromagnetic showers from the target. Since showers are soon absorbed by the magnet, the sign from the CMU closest to the main event vertex is rejected.

Appendix B

The straight track segments reconstructed by the PT provide track parameters projected in the horizontal plane (x, z) with z along the horizontal projection of the beam line and x parallel to the PT walls. Two segments on each side $j = 1, 2$ of the magnet arm are described by the angles ϕ_j that they make with axis x and by their distance $d_{0,j}$ to the reference frame origin.

These satisfy the Hessian normal form (see also Figures 2 and 3)

$$\left(\begin{pmatrix} x_j \\ z_j \end{pmatrix} - d_{0,j} \begin{pmatrix} \sin \phi_j \\ -\cos \phi_j \end{pmatrix} \right) \cdot \begin{pmatrix} \sin \phi_j \\ -\cos \phi_j \end{pmatrix} = 0 \quad (\text{B.1})$$

$\Delta\phi = |\phi_2 - \phi_1|$ is the deflection angle. If energy loss and multiple scattering are neglected the charged particle trajectory in the magnetic field is an arc of a circle tangent to both track segments at their magnet entry/exit points.

One defines, projected in the bending horizontal plane:

- **L** a direction vector on the line connecting *A*, the entry point of the upstream segment in the magnet and *B*, the exit point of the downstream segment.
- **a** a direction vector along the upstream segment and **b** a direction vector opposite to the downstream segment

If follows that

$$\mathbf{b} = \begin{pmatrix} z_2 - z_1 \\ x_1(z_2) - x_1(z_1) \end{pmatrix} \quad (\text{B.2})$$

$$\mathbf{a} = \begin{pmatrix} z_1 - z_2 \\ x_2(z_1) - x_2(z_2) \end{pmatrix} \quad (\text{B.3})$$

$$\mathbf{L} = \begin{pmatrix} z_2 - z_1 \\ x_2(z_2) - x_1(z_1) \end{pmatrix}. \quad (\text{B.4})$$

Where $x_j(z_i)$, defined by Eq. (B.1), is the x coordinate of the intersection point of track segment $j = 1, 2$ with respectively the front face of the magnet arm at $z = z_1$ and the back face at $z = z_2$ and

$$\alpha_1 = \arccos\left(\frac{\mathbf{b} \cdot \mathbf{L}}{b \cdot L}\right) \cdot s_1 \quad (\text{B.5})$$

$$\alpha_2 = \arccos\left(-\frac{\mathbf{a} \cdot \mathbf{L}}{a \cdot L}\right) \cdot s_2 \quad (\text{B.6})$$

where signs $s_{1,2}$ are given by

$$s_{1,2} = \frac{x_{1,2}(z_{2,1}) - x_{2,1}(z_{2,1})}{|x_{1,2}(z_{2,1}) - x_{2,1}(z_{2,1})|}, \quad (\text{B.7})$$

In order to calculate both angles (α_1 and α_2) the second parameter of the track segment fit (d_0) usually neglected for the charge sign determination is used. Assuming a perfect circular trajectory in the magnet (no energy loss, no multiple Coulomb scattering, homogeneous field) and infinite measurement precision, one has $\alpha_1 = \alpha_2$ and $\Delta\phi = \alpha_1 + \alpha_2$.

Acknowledgements

We thank CERN for the successful operation of the CNGS facility and INFN for the continuous support given to the experiment through its LNGS laboratory. We acknowledge funding from our national agencies: Fonds de la Recherche Scientifique-FNRS and Institut Interuniversitaire des Sciences Nucléaires

for Belgium, MoSES for Croatia, CNRS and IN2P3 for France, BMBF for Germany, INFN for Italy, JSPS, MEXT, QFPU (Global COE programme of Nagoya University) and Promotion and Mutual Aid Corporation for Private Schools of Japan for Japan, SNF, the University of Bern and ETH Zurich for Switzerland, the Russian Foundation for Basic Research (grant 12-02-12142 ofim, 15-02-01056_a), the Program for the Support of Leading Scientific School, contract SS 3110.2014.2, the Presidium of the Russian Academy of Sciences basic research program Fundamental Properties of Matter and Astrophysics, and the Ministry of Education and Science of the Russian Federation for Russia, and the National Research Foundation of Korea Grant No. 2011-0029457 for Korea. The authors would also like to thank Laura Vanhoefer for fruitful discussions and comments. B.B. and M.M. would also like to thank Ann Fielding for language support.

References

- [1] M. Guler, et al., Experiment proposal, CERN-SPSC-2000-028.
- [2] N. Agafonova, et al., Observation of a first ν_τ candidate event in the OPERA experiment in the CNGS beam, Phys. Lett. B 691 (2010) 138–145.
- [3] N. Agafonova, et al., Search for $\nu_\mu \rightarrow \nu_\tau$ oscillation with the OPERA experiment in the CNGS beam, New J. Phys. 14 (2012) 033017. doi: 10.1088/1367-2630/14/3/033017.
- [4] N. Agafonova, et al., Evidence for $\nu_\mu \rightarrow \nu_\tau$ appearance in the CNGS neutrino beam with the OPERA experiment, Phys.Rev. D89 (2014) 051102. doi:10.1103/PhysRevD.89.051102.
- [5] N. Agafonova, et al., Observation of tau neutrino appearance in the CNGS beam with the OPERA experiment, PTEP 2014 (10) (2014) 101C01. doi:10.1093/ptep/ptu132.
- [6] K. Olive, et al., Review of Particle Physics, Chin.Phys. C38 (2014) 090001. doi:10.1088/1674-1137/38/9/090001.
- [7] R. Acquafredda, et al., The OPERA experiment in the CERN to Gran Sasso neutrino beam, JINST 4 (2009) P04018. doi:10.1088/1748-0221/4/04/P04018.
- [8] B. Wonsak, Die Spurrekonstruktion für das Driftröhren-Myon-Spektrometer des Neutrino-Experimentes OPERA, Ph.D. thesis, University of Hamburg, (in German) (2007). URL <https://www-opera.desy.de/publications/Doktorarbeit-Bjoern-Wonsak.pdf>
- [9] R. Bailey, et al., CERN-SL-99-034-DI, INFN/AE-99/05 (1999), addendum to G. Acquistapace et al., CERN-98-02, INFN/AE-98/05 (1998). URL https://proj-cngs.web.cern.ch/proj-cngs/PDF_files/sl-99-034.pdf
- [10] N. Agafonova, et al., Limits on muon-neutrino to tau-neutrino oscillations induced by a sterile neutrino state obtained by OPERA at the CNGS beamarXiv:1503.01876.
- [11] R. Zimmermann, et al., The precision tracker of the OPERA detector, Nucl. Instrum. Meth. A555 (2005) 435–450. doi:10.1016/j.nima.2005.09.003.
- [12] N. Agafonova, et al., Measurement of the atmospheric muon charge ratio with the OPERA detector, Eur. Phys. J. C67 (2010) 25–37. doi:10.1140/epjc/s10052-010-1284-8.
- [13] R. Brun, et al., Technical report, CERN-DD/EE/84-1 (1987). URL <http://wwwasd.web.cern.ch/wwwasd/geant/>
- [14] N. Agafonova, et al., Study of neutrino interactions with the electronic detectors of the OPERA experiment, New J. Phys. 13 (2011) 053051. doi:10.1088/1367-2630/13/5/053051.
- [15] D. Autiero, The OPERA event generator and the data tuning of nuclear re-interactions, Nucl. Phys. Proc. Suppl. 139 (2005) 253–259. doi:10.1016/j.nucphysbps.2004.11.168.
- [16] J. Altegoer, et al., The NOMAD experiment at the CERN SPS, Nucl. Instrum. Meth. A404 (1998) 96–128. doi:10.1016/S0168-9002(97)01079-6.

- [17] R. Kalman, A new Approach to Linear Filtering and Prediction Problems, Journal of Basic Engineering 82.
- [18] N. Agafonova, et al., Measurement of the TeV atmospheric muon charge ratio with the complete OPERA data set, Eur.Phys.J. C74 (7) (2014) 2933. doi:10.1140/epjc/s10052-014-2933-0.
- [19] D. G. Michael, et al., The Magnetized steel and scintillator calorimeters of the MINOS experiment, Nucl. Instrum. Meth. A596 (2008) 190–228. doi:10.1016/j.nima.2008.08.003.
- [20] R. Zimmermann, Charge Sign Determination with the Precision Tracker of OPERA, OPERA public note 105 (2009).
URL <http://operaweb.lngs.infn.it/Opera/publicnotes/note105.pdf>